International Research Journal on Advanced Engineering Hub (IRJAEH)
e ISSN: 2584-2137
Vol. 02 Issue: 04 April 2024
Page No: 1010 - 1018
https://irjaeh.com
https://doi.org/10.47392/IRJAEH.2024.0141

Automated Liver Tumor Segmentation in DCE-MRI with 4D Deep Learning Integrating 3D CNNS and ConvLSTM

Sriram[1], Karthik[2]
[1,2]Department of Computer Science and Applications, Periyar Maniammai Institute of Science & Technology (Deemed to be University), Vallam, Thanjavur, Tamil Nadu, India.
Email ID: *sriramsubramaniyan114@gmail.com[1], karthikp@pmu.edu[2]*

Abstract
A state-of-the-art method for automatically segmenting liver tumours using Dynamic Contrast-Enhanced Magnetic Resonance Imaging (DCE-MRI) is shown in this study. This study is significant because it uses a 4D information deep learning model to tackle the hard problem of liver tumor segmentation. A combination of 3D CNNs and ConvLSTM networks, specifically built to capture spatial and temporal information inside the dynamic imaging sequence of DCE-MRI, is what the suggested model is all about. Utilizing diffusion-computed tomography (DCE-MRI) gives a lot of information vital for precise tumor segmentation by providing a complete picture of the vascular dynamics in the liver. The model makes use of spatial and temporal elements by combining 3D Convolutional Neural Networks (CNNs) with ConvLSTM networks; this allows for a more detailed comprehension of the changes that are happening over time. To overcome the difficulties caused by the constantly changing nature of DCE-MRI data, this integration of 4D information greatly improves the accuracy and consistency of liver tumor segmentation. Implementing and optimizing the suggested deep learning model are the main goals of this work. The training and calibration of the model to accurately capture liver tumor characteristics in dynamic imaging sequences is of utmost importance.

Keywords: *Liver Tumor, Deep Learning, LSTM, CNN, CT Scan, Liver Segmentation.*

1. Introduction
One of the leading causes of cancer-related mortality is liver cancer. Globally, hepatic cellular carcinoma (HCC) ranks third in terms of cancer-related mortality and ranks fifth among major malignant tumours [1]. It is the most prevalent form of primary liver cancer. Successful tumor excision requires early detection and treatment of HCC [2]. To better plan liver treatments, classify therapeutic responses, classify hepatic tumours, and estimate patient survival, it can be helpful to accurately segment tumours so volume-based quantitative information, including textural qualities, can be measured. Manual delineation is still used for liver tumor segmentation a lot of the time, although it's time-consuming, hard-working, and might vary from operator to operator [3-6]. For liver and lesion segmentation, many computer-aided approaches have been suggested, all based on conventional image processing algorithms [7-9]. Problems with automated segmentation arise from the fact that tumor form, appearance, and location can vary greatly, there are often no discernible borders, and contrast agents add noise to the mix [10-12]. Border leaking on hazy tumor borders [13-14] is a major issue with the previously stated approaches since they could only use restricted information, such as intensity information. In recent years, medical image processing has been considerably made easier because to the advent of deep learning. Brain tumor

International Research Journal on Advanced Engineering Hub (IRJAEH)
e ISSN: 2584-2137
Vol. 02 Issue: 04 April 2024
Page No: 1010 - 1018
https://irjaeh.com
https://doi.org/10.47392/IRJAEH.2024.0141

segmentation and prostate cancer detection are two examples of effective applications of deep Convolutional Neural Networks (CNNs) [15–17]. Deep learning has also found use in the imaging of healthy livers, the staging of liver fibrosis, the classification of liver statuses, the identification of hepatic tumours, and the differentiating of liver masses [18]. The data-driven algorithms that make up deep learning allow for the automatic capture of high-level features from photographs and performance improvements in these areas [19]. Deep learning has also shown to be quite effective in liver tumour segmentation, as all of the top algorithms in the 2017 Liver Tumour Segmentation (LiTS) competition used it [20]. The main contribution of the paper:

- Image denoising using Non adaptive threshold
- Segmentation using fused U-Net
- Feature extraction using Histogram of Oriented Gradients
- Classification using 3D Convolutional Neural Networks (CNN) with Convolutional Long Short-Term Memory

Following is the outline for the rest of the article. Section 2 covers a number of liver tumor diagnostic methodologies, written by several writers. In Section 3, we can see the suggested model. Presented in Section 4 are the investigation's conclusions. Results and future work are discussed in Section 5.

1.1. Motivation of the Paper

By presenting a 4D data deep learning model, this study tackles the difficulties of liver tumor segmentation in DCE-MRI techniques. A combination of 3D CNN and ConvLSTM networks allows the model to take advantage of the dynamic nature of DCE-MRI while capturing spatial and temporal characteristics. Improving accuracy in areas where current approaches are inadequate is the driving force. In line with the increasing need for clinical accuracy and with the goal of improving patient outcomes, the study advances accurate tumor segmentation in medical imaging by offering a strong answer.

2. Background Study

- Bakrania et al. [1] investigate the revolutionary function of ML models in the clinical detection of primary and metastasized liver tumours. Their in-depth research sheds light on how AI might change the face of diagnosis and provide new ways of thinking about patient care. The research highlights the need of incorporating sophisticated technologies into clinical practice by deciphering the models' impacts; this will allow for more precise and faster diagnosis.
- Esposito et al. [2] provide a ground-breaking method for evaluating primary human liver cancer cells using Raman spectroscopy supported by artificial intelligence. Their work demonstrates how AI might enhance diagnostic capacities by offering deep insights into the molecular makeup of malignant cells. New possibilities for accurate and non-invasive cancer detection were presented by this study, which uses Raman spectroscopy in conjunction with machine learning.
- Gavini and Lakshmi [3] put forth a novel long short-term memory (LSTM) model that uses convolutional neural networks (CNNs) to predict the grade of liver tumours in CT scans. An essential part of therapy planning was appropriately assessing tumours, and their study shows that deep learning algorithms work well for this task. With the use of associated characteristics taken from CT scans, the model was able to attain a high level of accuracy, giving doctors important data for individualizing patient treatment.
- Hendi et al. [4] explore the use of deep learning methods for sub typing and predicting liver disorders using an adaptive strategy. The significance of personalized medicine techniques in enhancing patient outcomes was highlighted by their research. Improved methods of illness management were a direct result of this study's

International Research Journal on Advanced Engineering Hub (IRJAEH)
e ISSN: 2584-2137
Vol. 02 Issue: 04 April 2024
Page No: 1010 - 1018
https://irjaeh.com
https://doi.org/10.47392/IRJAEH.2024.0141

focus on personalizing deep learning models for each patient.

- Kang et al. [5] concentrate on applying AI to forecast the amounts of safe liver resections for large keratectomy operations. By improving resection planning for the benefit of both patients and surgeons, their work tackles an important facet of liver surgery. This project aims to improve surgical decision-making and patient outcomes by incorporating AI algorithms into preoperative planning.
- Khan et al. [6] release a deep neural network that can detect liver cancer in several classes using multiple input modalities. Their work was groundbreaking because it improves diagnosis accuracy by combining data from several sources. Improved liver cancer diagnosis and subsequent treatment choices were made possible by the suggested model's incorporation of supplementary data from many modalities.

2.1. Problem Definition

The precise segmentation of liver tumours using Dynamic Contrast-Enhanced Magnetic Resonance Imaging (DCE-MRI) is the subject of this study. Due to the ever-changing nature of DCE-MRI data, current approaches struggle to capture the intricacies of liver tumor characteristics. To traverse these obstacles, the research suggests a new 4D data deep learning model that merges 3D CNN with ConvLSTM networks. Using spatial and temporal data collected from DCE-MRI dynamic imaging sequences, we want to improve tumor segmentation accuracy and reliability. Evaluating the suggested model's effectiveness in clinical settings and putting it into practice are other areas of emphasis in the study.

3. Materials and Methods

The experimental setup and techniques used in the mentioned papers are outlined in the materials and methods section. Research methods, including data collecting, model construction, and analytic approaches, are described in great depth. In order to grasp the scientific rigor of the presented results and to replicate the experiments, this section is designed to be a guide.

3.1. Dataset Collection

The dataset was collected from Kaggle web site https://www.kaggle.com/datasets/andrewmvd/lits-png among male cancers, liver cancer ranks fifth, whereas among female cancers, it is ninth. More than 840,000 new cases were reported in 2018, as shown in Figure 1.

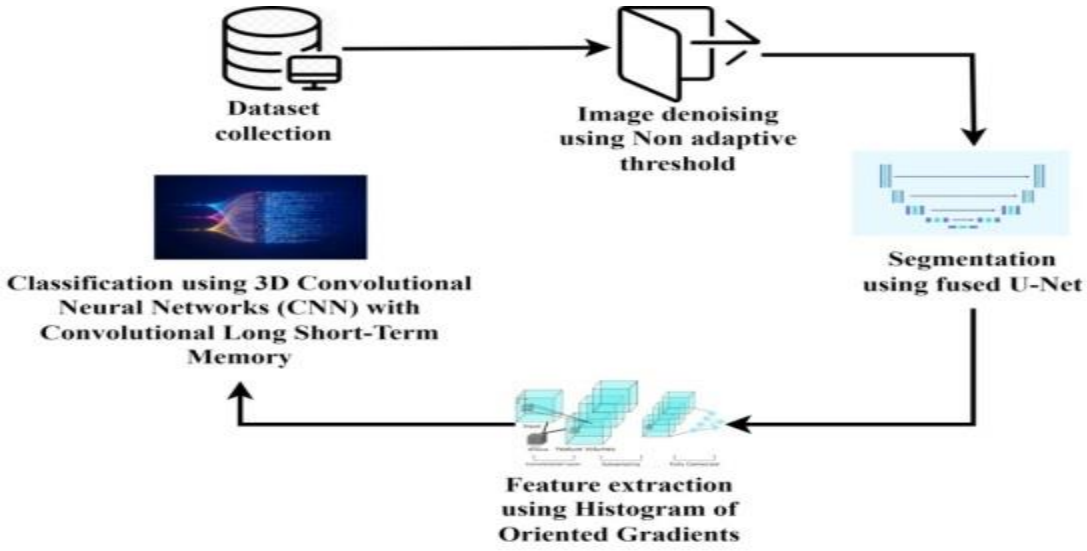

Figure 1 Overall Architecture

International Research Journal on Advanced Engineering Hub (IRJAEH)
e ISSN: 2584-2137
Vol. 02 Issue: 04 April 2024
Page No: 1010 - 1018
https://irjaeh.com
https://doi.org/10.47392/IRJAEH.2024.0141

3.2. Image Denoising using Non-adaptive Threshold

An easy method for picture denoising is non-adaptive thresholding, which involves applying a constant threshold value consistently throughout the whole image to determine whether pixels are signals or noise. In this approach, the noise properties and the intended denoising level are used to determine a threshold value. Then, pixels are classified as either signal or noise depending on how intense they are in comparison to the threshold. Denoising methods, such median or Gaussian filtering, are then used to modify or replace the noise pixels. Despite its computing efficiency and ease of implementation, non-adaptive thresholding cannot work as well when faced with complicated picture structures or situations where the properties of the noise fluctuate geographically. Our goal in writing this paper was to build upon Asymptotically, the time required to locate broken objects in a noisy setting can be limited, and a maximum number of tests can be determined (Zhao, Z. et al. 2023). The amount of encoding tests and the time needed for decoding in threshold group testing (TGT) with a gap can be decreased by building a matrix. To demonstrate this point, we use Algorithm 1 to the (n, d _, u; z]-disjunction matrix shown in of. There must be numbers such that $(e-r)\binom{x-r}{d+1}$ holds. Figure it out. S is the defective set and z is the positive integer; we'll keep things simple. A non-adaptive approach can successfully identify set using just$(x, e-i, r; y]$ tests in a $(x, e-i, r; y]-TGT$ model with a maximum of $(x, e-i, r; y]$ incorrect outcomes, where the decoding difficulty is:

$$O\left(g(x, e-i, r; y] \times r\left(\binom{x}{r}+(e-r)\binom{x-r}{d+1}\binom{e-1}{g}\binom{e}{r}\right)\right) \text{--- (1)}$$

3.3. Segmentation using Fused U-Net

To increase the accuracy of segmentation, Fused U-Net makes use of a modified U-Net architecture that includes many input modalities or characteristics. U-Nets are known for their effective collection of spatial information at various scales, to its encoder-decoder structure with skip links referred by Weimin, W. et al. (2024). Fused U-Net takes the original picture as input and fuses it with other modalities, such as complementing feature maps or other imaging modalities. The network's capacity to detect various picture features is improved by this data fusion, which ultimately leads to better and more accurate segmentation outcomes. To identify objects or areas of interest in input pictures, the network learns during training to efficiently combine data from several modalities or characteristics. With its ability to fuse data from numerous sources, Fused U-Net has shown effective in medical picture segmentation tasks. This is especially true in difficult situations involving structures with unclear borders or complicated structures. The Fused U-Net architecture features bypass channels connecting the encoder and decoder, and a thick convolution block with several convolution layers and concatenation layers preceding each convolution layer serves as the backbone. It is in the concatenation layer that the input and output of the preceding and current convolution layers are combined. With the information about the activation function convolution block (D), the maximum pooling operation (P), and the up sampling function (T), we can use Equation (2) to getx^{ik}.

$$x^{ij}=\begin{cases} D\left(p(x^{i-1j})\right) & j=0 \\ D\left(p\left([x^{ik}]^{j-1}{}_{k=0}T(x^{i+1j-1})\right]\right) & j>0 \end{cases} \text{------- (2)}$$

The input to Layer 0 comes exclusively from the encode layer before it, whereas the input to Layer j > 0 comes from the j levels before it in the same skip route and also from the lower skip pathway's up-sampled output $T\left(x^{i+1j-1}\right)$. Fused U-Net design has several benefits over regular U-Net, including improved segmentation accuracy and fine-grained feature preservation. Objects of varying sizes can be handled via the hierarchical Fused U-Net's skip connections.

3.4. Feature Extraction using Histogram of Oriented Gradients

A well-known method in computer vision for representing the local gradient information in an

International Research Journal on Advanced Engineering Hub (IRJAEH)
e ISSN: 2584-2137
Vol. 02 Issue: 04 April 2024
Page No: 1010 - 1018
https://irjaeh.com
https://doi.org/10.47392/IRJAEH.2024.0141

image is feature extraction using Histogram of Oriented Gradients (HOG). In this method, the picture is partitioned into smaller spatial areas called cells, and the direction and amplitude of the gradients inside each cell are calculated. The distribution of gradient directions inside the cell is quantified by constructing a histogram of gradient orientations using these gradient values. To better capture the spatial interactions between cells, it is common practice to aggregate nearby cells into bigger blocks. The histograms of these blocks are then normalized to make them more resistant to variations in light and contrast. The resultant HOG feature descriptor is well-suited for applications like object identification, recognition, and classification as it contains details about the image's local edge or texture patterns. Situations where an object's form or texture discriminates across classes or categories are ideal for HOG features. Distributions of local intensity gradients or edge orientations can often accurately describe the form and look of local objects, even when exact information about the gradient or edge placements is not known. This statement defines the HOG approach, which has an extensive history of application in human identification and has been used in its mature version in Scale Invariant Features Transformation. By integrating gradient directions across a tiny spatial region known as a "cell" pixel, the HOG descriptor is built upon. Afterwards, a 1D histogram is built, and the features vector that will be considered later is the product of their combination. Let L denote the image to be examined as a grayscale (intensity) function. We use the following rule to find the x and y gradient directions in each pixel after we divide the image into cells of size N pixels:

$$\theta_{x,y} = tan^{-1} \frac{L(x,y+1)-L(x,y-1)}{L(x+1,y)-L(x-1,y)} \text{ -------- (3)}$$

The following is the normalization process for the single HOG feature vector h that is created by merging the normalized block features:

$$h \leftarrow \frac{h}{\sqrt{||h||^2+\epsilon}} \text{ ---------- (4)}$$

$$h_n \leftarrow \min(h_n, t) \text{ ---------- (5)}$$

$$h \leftarrow \frac{h}{\sqrt{||h||^2+\epsilon}} \text{ ---------- (6)}$$

HN represents the nth element of h, whereas is a positive cutoff (= 0:2). If large gradients had an outsized impact, they would obscure every other feature in the image. The number of cell histograms relative to blocks in the resulting HOG characteristic is four times higher.

3.5. Classification using 3D Convolutional Neural Networks (CNN) with Convolutional Long Short-Term Memory

Classification using 3D CNNs with ConvLSTM networks is an effective method for looking at spatiotemporal data, especially for applications that include volumetric or video data. 3D convolutional neural networks (CNNs) are advancement over their 2D predecessors, specifically built to handle data in three dimensions, including medical volumetric pictures or video frames. 3D convolutional layers make up these networks, and they capture spatial connections in the input data by extracting spatial properties over the whole volume. The model can detect temporal relationships in sequential data by using 3D CNNs with ConvLSTM layers. Like regular LSTM cells, convLSTM cells have a memory cell and gates to regulate the flow of data. Nevertheless, ConvLSTM enables the network to learn spatiotemporal patterns directly from the input by performing the operations in a convolutional fashion. The 3D convolutional layers allow the ConvLSTM model to learn how to extract spatial characteristics from the input data in each frame or volume during training. After that, the ConvLSTM layers get the features that were extracted and use them to record the dependencies that occurred over time in successive frames or volumes. This improves the model's classification performance by letting it learn and reflect the data's dynamics and mobility more effectively. An example of a deep learning model is a convolutional neural network, which can be used to analyze images. Convolutional layers with filters, batch normalization layers, pooling layers, non-linear activations, and FC layers are some of the many

International Research Journal on Advanced Engineering Hub (IRJAEH)
e ISSN: 2584-2137
Vol. 02 Issue: 04 April 2024
Page No: 1010 - 1018
https://irjaeh.com
https://doi.org/10.47392/IRJAEH.2024.0141

processing steps that Convolutional Long Short-Term Memory convolutional neural networks (CNNs) go through while processing images. The complete connection weights and convolution filter weights are the trainable parameters of a CNN model with Convolutional Long Short-Term Memory. The proposed convolutional neural network (CNN) model for brain tumor classification includes two feed forward (FC) layers (fc_1 and fc_2) and five convolutional (conv_1–conv_5) layers, as shown in Table 3.1. The proposed CNN model, which makes use of Convolutional Long Short-Term Memory, is capable of handling 256x256 images to its 256x256 input layer. A convolution layer uses a series of filters, one after another, to collect various activations from the input image. The matrix $y(m,n)$ that results from the linear convolution of a size FxF filter $k(m,n)$ with an image $x(m,n)$ is,

$$y(m,n) = \sum_{i=-\frac{F}{2}}^{\frac{F}{2}} \sum_{j=-\frac{F}{2}}^{\frac{F}{2}} x(i,j)k(m-i,n-j) \text{ --- (7)}$$

The input volume with dimensions $(X1, Y1, Z1)$ becomes a volume with dimensions $(X2, Y2, K)$ after applying K filters. The formulas for X2 and Y2 are as follows,

$$X_2 = \frac{X_1 - F + 2P}{S} + 1 \text{ -------- (8)}$$

$$Y_2 = \frac{Y_1 - F + 2P}{S} + 1 \text{ ------- (9)}$$

According to this plan, they are both the one and two people involved. Each batch normalization layer is followed by an activation layer using ReLU. Each ReLU operation is followed by a max-pooling.

Algorithm 1: CNN with Convolutional Long Short-Term Memory

Input:

- A 4D tensor representing sequential volumetric data, where dimensions correspond to batch size, depth, height, and width.

Steps:

1. Input Preparation: Preprocess input data to ensure uniform dimensions and format. Normalize input data if necessary.

$$y(m,n) = \sum_{i=-\frac{F}{2}}^{\frac{F}{2}} \sum_{j=-\frac{F}{2}}^{\frac{F}{2}} x(i,j)k(m-i,n-j)$$

2. Model Construction: Define the architecture of the 3D CNN with ConvLSTM model, specifying the number and size of convolutional layers, LSTM layers, and fully connected layers.
3. Model Compilation: Compile the model by specifying the optimizer, loss function, and evaluation metrics.

$$X_2 = \frac{X_1 - F + 2P}{S} + 1$$

4. Training: Train the model on a labeled dataset of sequential volumetric data, adjusting the model parameters using back propagation and optimization algorithms to minimize the loss function.

Output:

- Probability distribution over the classes for each input sequence.

4. Results and Discussion

The study's findings are reported and examined in depth in the results and discussion section. The purpose of this part is to analyze the results of the experiments, assess how well the techniques that were suggested worked, and talk about what those results mean in relation to the goals of the study.

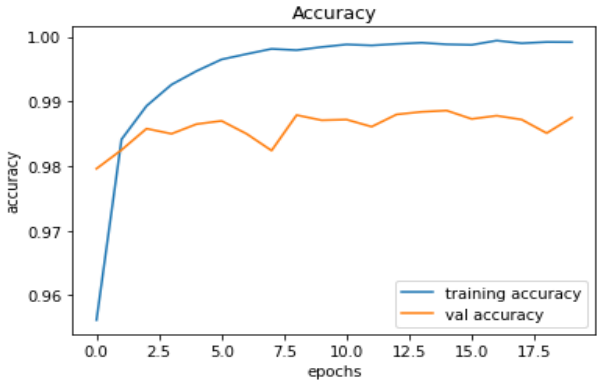

Figure 2 Training Accuracy Comparison Chart

The Figure 2 shows training accuracy comparison chart the x axis shows epochs and the y axis shows accuracy.

International Research Journal on Advanced Engineering Hub (IRJAEH)
e ISSN: 2584-2137
Vol. 02 Issue: 04 April 2024
Page No: 1010 - 1018
https://irjaeh.com
https://doi.org/10.47392/IRJAEH.2024.0141

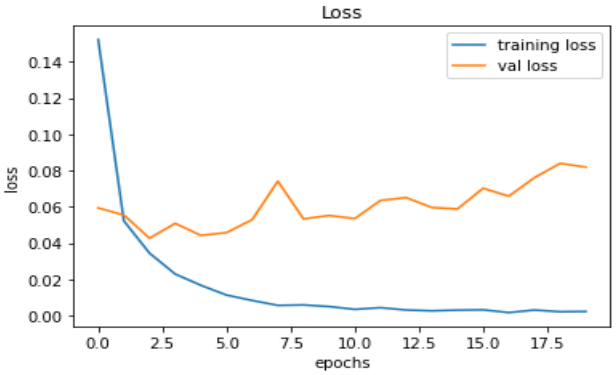

Figure 3 Training Loss

The Figure 3 shows training loss value comparison chart the x axis shows epochs and the y axis shows training loss and Figure 4 shows the denoisied image.

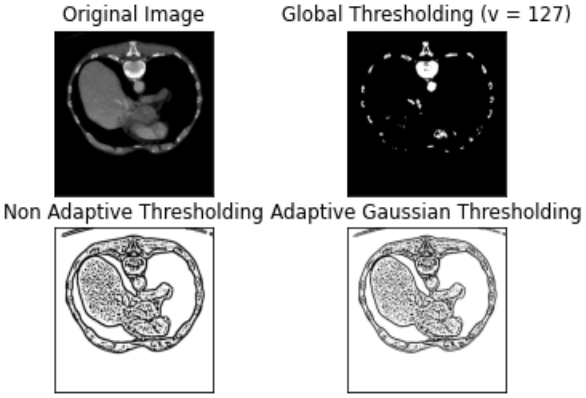

Figure 4 Denoisied Image

Table 1 Classification Performance Metrics Comparison

	Algorithm	Accuracy	Precision	Recall	F-measure
Existing methods	SVM	94.32	90.74	91.37	90.21
	LSTM	95.24	92.54	92.14	93.00
	CNN	96.37	95.00	94.25	95.00
Proposed methods	Proposed	98.22	97.32	97.10	96.92

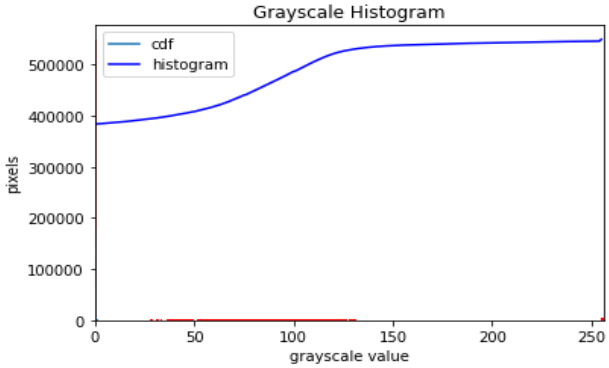

Figure 5 Grayscale Histogram

The Figure 5 shows grayscale histogram chart the x axis shows grayscale value and the y axis shows pixels, and Figure 6 shows the feature values chart.

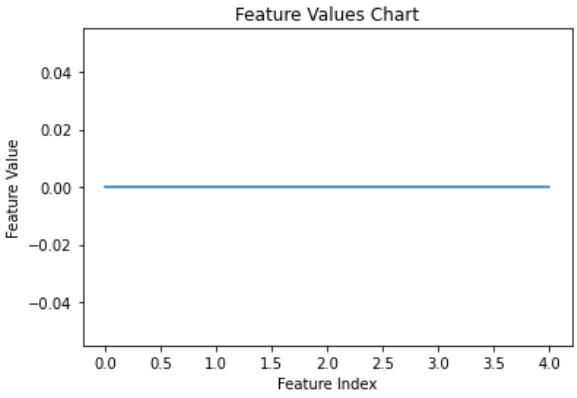

Figure 6 Feature Values Chart

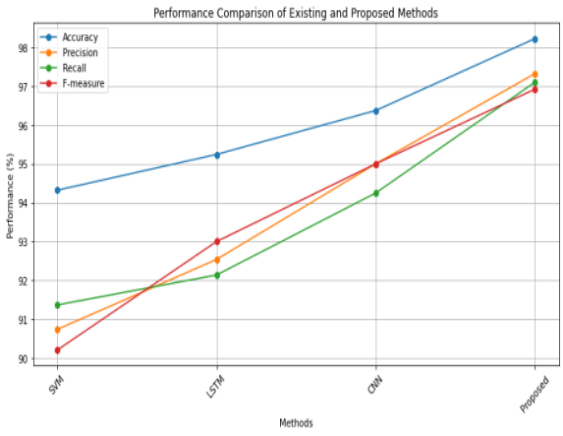

Figure 7 Performance Metrics Comparison Chart

International Research Journal on Advanced Engineering Hub (IRJAEH)
e ISSN: 2584-2137
Vol. 02 Issue: 04 April 2024
Page No: 1010 - 1018
https://irjaeh.com
https://doi.org/10.47392/IRJAEH.2024.0141

The suggested technique surpasses current methods in every assessment parameter, including accuracy, precision, recall, and F-measure, as shown in Table 1 and Figure 7. In particular, compared to SVM (94.32%), LSTM (95.24%), and CNN (96.37%), the suggested technique attains a much greater accuracy of 98.22%. It also shows less false positives (97.32%) and greater accuracy (97.34%) than SVM (90.74%), LSTM (92.54%), and CNN (95.00%). Better capacity to recognize true positives is shown by the suggested method's recall (97.10%), which is much greater than that of SVM (91.37%) and LSTM (92.14%). Furthermore, the suggested strategy outperforms SVM (90.21%), LSTM (93.000%), and CNN (95.00%) in terms of F-measure, suggesting a balanced performance in terms of recall and accuracy. When compared to other methods, these results demonstrate how much better the suggested technique is at producing trustworthy classifications.

Conclusion

Finally, this study presents a cutting-edge method for automated liver tumor segmentation that is specifically designed for DCE-MRI imaging. Specifically for dynamic imaging sequences, the research tackles the challenges of liver tumor segmentation by using a 4D information deep learning model that combines 3D CNN with ConvLSTM networks. The suggested model incorporates both spatial and temporal data, which greatly improves tumor segmentation accuracy, while DCE-MRI gives a complete picture of the vascular dynamics in the liver. The study's basic goals, which revolve on optimizing the model and evaluating its performance, highlight its dedication to improving tumor segmentation methods. This study adds to the body of knowledge in medical imaging by showing how the suggested strategy might improve upon or perhaps replace current practices. The increasing need for accuracy in healthcare settings is well-suited to a 4D information deep learning model that incorporates both spatial and temporal variables. Positive effects on patient outcomes can result from the study's novel methodology, which shows potential in enhancing diagnostic and therapeutic capacities for liver tumours.

Reference

[1]. Bakrania, A., Joshi, N., Zhao, X., Zheng, G., & Bhat, M. (2023). Artificial intelligence in liver cancers: Decoding the impact of machine learning models in clinical diagnosis of primary liver cancers and liver cancer metastases. Pharmacological Research, 189, 106706.

[2]. Esposito, C., Janneh, M., Spaziani, S., Calcagno, V., Bernardi, M. L., Iammarino, M., ... & Cusano, A. (2023). Assessment of Primary Human Liver Cancer Cells by Artificial Intelligence-Assisted Raman Spectroscopy. Cells, 12(22), 2645.

[3]. Gavini, V., & Lakshmi, G. J. (2022, December). Liver Tumor Grade Detection using CNN Based LSTM Model with Corelated Feature Set from CT Images. In 2022 International Conference on Automation, Computing and Renewable Systems (ICACRS) (pp. 843-850). IEEE.

[4]. Hendi, A. M., Hossain, M. A., Majrashi, N. A., Limkar, S., Elamin, B. M., & Rahman, M. (2024). Adaptive Method for Exploring Deep Learning Techniques for Subtyping and Prediction of Liver Disease. Applied Sciences, 14(4), 1488.

[5]. Kang, C. M., Ku, H. J., Moon, H. H., Kim, S. E., Jo, J. H., Choi, Y. I., & Shin, D. H. (2024). Predicting Safe Liver Resection Volume for Major Hepatectomy Using Artificial Intelligence. Journal of Clinical Medicine, 13(2), 381.

[6]. Khan, R. A., Fu, M., Burbridge, B., Luo, Y., & Wu, F. X. (2023). A multi-modal deep neural network for multi-class liver cancer diagnosis. Neural Networks, 165, 553-561.

[7]. Kim, S., & Lee, E. (2023). A deep attention LSTM embedded aggregation network for multiple histopathological images. PLoS One, 18(6), e0287301.

International Research Journal on Advanced Engineering Hub (IRJAEH)
e ISSN: 2584-2137
Vol. 02 Issue: 04 April 2024
Page No: 1010 - 1018
https://irjaeh.com
https://doi.org/10.47392/IRJAEH.2024.0141

[8]. Kucukkaya, A. S., Zeevi, T., Chai, N. X., Raju, R., Haider, S. P., Elbanan, M., ... & Chapiro, J. (2023). Predicting tumor recurrence on baseline MR imaging in patients with early-stage hepatocellular carcinoma using deep machine learning. Scientific Reports, 13(1), 7579.

[9]. Li, G., Zhang, X., Song, X., Duan, L., Wang, G., Xiao, Q., ... & Bai, S. (2023). Machine learning for predicting accuracy of lung and liver tumor motion tracking using radiomic features. Quantitative Imaging in Medicine and Surgery, 13(3), 1605.

[10]. Li, Y., & Hu, D. (2021, October). Liver Tumor Segmentation Based on Three-Channel Cascaded SEU-Nets and C-LSTM. In 2021 13th International Conference on Wireless Communications and Signal Processing (WCSP) (pp. 1-5). IEEE.

[11]. Manjunath, R. V., Ghanshala, A., & Kwadiki, K. (2024). Deep learning algorithm performance evaluation in detection and classification of liver disease using CT images. Multimedia Tools and Applications, 83(1), 2773-2790.

[12]. Ragab, M., & Alyami, J. (2023). Stacked Gated Recurrent Unit Classifier with CT Images for Liver Cancer Classification. Computer Systems Science & Engineering, 44(3).

[13]. Saumiya, S., & Franklin, S. W. (2024). Unified automated deep learning framework for segmentation and classification of liver tumors. The Journal of Supercomputing, 80(2), 2347-2380.

[14]. Weimin, W. A. N. G., Yufeng, L. I., Xu, Y. A. N., Mingxuan, X. I. A. O., & Min, G. A. O. (2024). Enhancing Liver Segmentation: A Deep Learning Approach with EAS Feature Extraction and Multi-Scale Fusion. International Journal of Innovative Research in Computer Science & Technology, 12(1), 26-34.

[15]. Wu, Q., Yu, J., Zhang, M., Xiong, Y., Zhu, L., Wei, B., ... & Du, Y. (2024). Serum lipidomic profiling for liver cancer screening using surface-assisted laser desorption ionization MS and machine learning. Talanta, 268, 125371.

[16]. Xia, T., Zhao, B., Li, B., Lei, Y., Song, Y., Wang, Y., ... & Ju, S. (2024). MRI-Based Radiomics and Deep Learning in Biological Characteristics and Prognosis of Hepatocellular Carcinoma: Opportunities and Challenges. Journal of Magnetic Resonance Imaging, 59(3), 767-783.

[17]. Yi, X., Wen, B., Ji, S., Saltzman, A. B., Jaehnig, E. J., Lei, J. T., ... & Zhang, B. (2024). Deep learning prediction boosts phosphoproteomics-based discoveries through improved phosphopeptide identification. Molecular & Cellular Proteomics, 23(2).

[18]. Zhang, Y., Dai, X., Tian, Z., Lei, Y., Wynne, J. F., Patel, P., ... & Yang, X. (2023). Landmark tracking in liver US images using cascade convolutional neural networks with long short-term memory. Measurement Science and Technology, 34(5), 054002.

[19]. Zhao, Z., Tian, Y., Yuan, Z., Zhao, P., Xia, F., & Yu, S. (2023). A machine learning method for improving liver cancer staging. Journal of Biomedical Informatics, 137, 104266.

[20]. Zheng, R., Wang, Q., Lv, S., Li, C., Wang, C., Chen, W., & Wang, H. (2022). Automatic liver tumor segmentation on dynamic contrast enhanced mri using 4D information: Deep learning model based on 3D convolution and convolutional lstm. IEEE Transactions on Medical Imaging, 41(10), 2965-2976.